Uplink Access Protocol in IEEE 802.11ac

M. Zulfiker Ali, *Student Member, IEEE*, Jelena Mišić, *Fellow, IEEE*, and Vojislav B. Mišić, *Senior Member, IEEE*

***Abstract*— The IEEE 802.11ac amendment enhances WLAN throughput by exploiting the spatial diversity of the antennas in a multi-user multi-input multi-output downlink transmission. Still, network resources remain under-utilized in uplink transmission due to single-user communication. In this paper, we propose an access point-controlled MAC protocol (A-MAC) that enables simultaneous transmissions from multiple STAs in uplink. The protocol uses the EDCA channel access technique to initiate multi-user transmission and the OFDMA method to transmit multiple RTSs simultaneously. It also introduces the explicit channel sounding technique by using dedicated OFDM subcarrier blocks for each user. Performance measurement shows that network throughput of the A-MAC is 150% higher than that of a single uplink transmission, thanks to the availability of concurrent multiple RTS transmissions in the uplink. The proposed protocol shortens the backoff time by up to 50% for all traffic categories due to concurrent multiple transmissions and thus enhances the battery life of the nodes. We observe that although the smaller backoff window of high-priority traffic category enhances the network throughput, higher intensity of high-priority traffic drives the network faster to saturation. Furthermore, better network stability and fairness among different traffic categories can be achieved when the dominant traffic has low priority.**

***Index Terms*— Wireless communications, access protocols, IEEE 802.11ac, multiuser uplink access.**

I. Introduction

IEEE 802.11 protocol is continuously evolving to keep pace with the growing need for high speed broadband multimedia communication. IEEE 802.11ac is a recent amendment that supports point-to-multipoint communication in the downlink (DL) using pioneering multi-input multi-output (MIMO) technique. DL-MIMO increases the network throughput by allowing transmission to maximum four STAs simultaneously using spatial multiplexing. The protocol still uses one-to-one communication in the uplink direction which keeps the abundant resources in AP under-utilized. In fact, the throughput of WLANs scales linearly with the multi packet reception (MPR) capability of the channel [1]. The technical challenges of multiple concurrent uplink transmissions require the AP receiver to perform per-user channel estimation, and carrier frequency offset estimation due to RF mismatches between STAs and AP [2]. Without precise channel state information (CSI), space diversity through beamforming technique cannot be utilized in the uplink due to overlapping of multiple transmitting signals at AP.

The development of Multiuser Detection (MUD) techniques like Zero Forcing (ZF) or Minimum Mean Squared Error (MMSE), for high speed data [3], [4], and blind detection algorithms such as Constant Modulus (CM) or Finite Alphabet (FA), for low rate data [5], [6], allows concurrent transmissions of multiple STAs in the uplink to be successfully decoded by the AP when the CSI between STA and AP is known and the number of transmissions does not exceed the number of receiver antennas. To successfully decode all transmissions, MIMO receiver must first acquire knowledge of all channels between any transmitting/receiving antenna pairs. In IEEE 802.11ac protocol, channel state information is obtained by the training bits in the preamble. However, to determine channel state effectively, preamble transmission must be in a clear channel state which means that, during multiple uplink transmission, interference-free preamble detection cannot be guaranteed. Therefore, an explicit channel sounding technique is required for uplink MU-MIMO transmission.

The benefits of these physical layer techniques can be fully exploited by designing a suitable MAC protocol for uplink multi-user transmission. Task Group AX (TGax) is working towards developing IEEE 802.11ax protocol by 2019 that will provide enhanced throughput and power efficiency in dense WiFi deployment environment [7], [8]. The new specification addresses the spectral inefficiency in existing protocol by including schedule based MU-MIMO and MU-OFDMA techniques to perform multi-user uplink transmission for high efficiency (HE) devices. However, the complete adoption of HE WLAN protocol is likely to take place over a period of time to offset the deployment cost. To ensure the coexistence of non-HE devices during the transition period, EDCA-based single user transmission will remain the basic access technique and single point of spectral inefficiency for non-HE devices in uplink. In this paper we discuss an EDCA-based uplink transmission technique for non-HE devices that allows multi-user transmission to improve spectral efficiency in a coexistent WLAN network. We propose an Access Point-controlled contention based MAC protocol (A-MAC) and explicit channel sounding technique that allow multi-user concurrent uplink transmission within IEEE 802.11ac framework keeping compatibility with the downlink MU-MIMO technique. The proposed protocol is a step towards implementing the desired throughput enhancement using concurrent multiple uplink transmissions and MIMO-OFDMA techniques. The major contributions of this paper are:

Manuscript received June 14, 2017; revised October 22, 2017, January 18, 2018, January 25, 2018, April 8, 2018, and May 30, 2018; accepted June 4, 2018. Date of publication June 15, 2018; date of current version August 10, 2018. This work was supported by the National Science and Engineering Research Council, Canada, through Discovery Grants-Individual program. The associate editor coordinating the review of this paper and approving it for publication was W. Chen. *(Corresponding author: Jelena Mišić.)*

The authors are with Ryerson University, Toronto, ON M5B 2K3, Canada (e-mail: mzulfiker.ali@ryerson.ca; jmisic@ryerson.ca; vmisic@ryerson.ca).

Color versions of one or more of the figures in this paper are available online at http://ieeexplore.ieee.org.

Digital Object Identifier 10.1109/TWC.2018.2845410

TABLE I
LIST OF ABBREVIATIONS USED IN THE PAPER

Abbreviation	Description
AC	Access Category
AIFS	Arbitration Inter-frame Spacing
A-MSDU	Aggregate MSDU
BO	Backoff
CSI	Channel State Information
CTS	Clear to Send
CW	Contention Window
DCF	Distributed Coordination Function
DIFS	DCF Inter-frame Spacing
EDCA	Enhanced Distributed Channel Access
EDCAF	EDCA Function
G-ACK	Group ACK
G-CTS	Group CTS
HPG	High Priority traffic Group
LPG	Low priority traffic Group
MIMO	Multiple Input Multiple Output
MPDU	MAC Protocol Data Unit
MPR	Multi Packet Reception
MSDU	MAC Service Data Unit
MU	Multi User
NDP	Null Data Packet
NDPA	NDP Announcement
PPDU	PHY Protocol Data Unit
RTS	Ready to Send
SIFS	Short Inter-frame Spacing
VHT	Very High Throughput
TXOP	Transmission opportunity
AIFSN	AIFS number Throughput
LST	Laplace-Stieltjes transform
NDP	Null Data Packet
PGF	Probability generating function
MU-MIMO	Multi-user MIMO
DL-MIMO	Downlink MIMO
OFDMA	Orthogonal frequency division multiple access
A-MPDU	Aggregate MPDU
STA	Station
AP	Access point

- To the best of our knowledge, this is the first uplink protocol using MU-MIMO and OFDMA techniques and the first to take into consideration different priority traffic categories.
- We introduce explicit channel sounding technique by using dedicated subcarrier blocks.
- We develop an analytical model using queuing model and Markov chain model to evaluate the performance of the proposed A-MAC.
- We evaluate the performance metrics of proposed A-MAC protocol for both uniformly and non-uniformly varying packet arrival rates for different priority categories.
- We develop the stable operating criterion for the network for varying traffic conditions.
- The proposed protocol provides a green solution by reducing the backoff time and thereby increasing the efficiency of the network.

The rest of the paper is organized as follows: In Section II we have discussed the related works followed by the proposed A-MAC protocol in Section III. The analytical model is discussed in Section IV. The numerical results are discussed in Section V followed by conclusion in Section VI. Tables I and II list major abbreviations and variables, respectively, used in the paper.

TABLE II
LIST OF KEY VARIABLES USED IN THE PAPER

Parameter	Description
k	Priority index
n	Number of STAs
p_{rts}	RTS Tx probability of a STA
p_{cts}	CTS Rx probability of a STA
π_0	Prob of queue of a STA empty
τ	Transmission probability of a STA
$\theta[i]$	Prob. of i packets in a burst
$fm[t]$	CTS Rx prob of 1 of t secondary STAs
fmu	Mean CTS Rx prob of a secondary STA
ψ_μ	Prob. of μ bursts Tx during TXOP
f	Time slot idle probability
M	TXOP limit of a STA
ps_l	Successful medium access prob
psf_l	Freezing counter restart prob.
γ	Successful packet Tx prob
δ_r	No RTS error prob
δ_c	No CTS error prob
v	Probabilistic backoff duration
v^+	Probabilistic residual backoff duration
g	Backoff counter decrement prob
M_k	TXOP limit of a STA
V	PGF of v
$B^*(s)$	LST of V
V^+	PGF of v^+
$B^{+*}(s)$	LST of V^+

II. RELATED WORK

The concept of multipacket reception in WLAN was first introduced in [9] and central coordinator scheduled MPR protocols were proposed in [10] and [11]. The first DCF-based MPR protocol [12] assumes the transmission of multiple RTSs at the beginning of transmission. However, due to random access nature in EDCA channel access, it is unlikely that multiple STAs pick the same backoff counter value and send RTS at the same time, in which case the channel is unavoidably under-utilized most of the time and the performance of the protocol will be poor. On the other hand, in a densely concentrated network, we may expect that the number of contending STAs to simultaneously transmit RTSs may easily exceed the number of antennas in the AP. As the protocol does not have any control on the number of RTSs, there is higher chance of collisions, esp. in high load condition.

The MAC protocol proposed in [13] requires a major change in the IEEE 802.11 protocol. The inclusion of multiple RTS/CTS during random access period increases the overhead burden to the protocol and, consequently, reduces network throughput and efficiency. The protocol also assumes single transmission opportunity (TXOP) duration for all traffic categories which either benefits low priority traffic category or penalizes the high priority traffic category. A spatial multiple access (SAM) protocol proposed in [14] for uplink asynchronous data transmission requires the stations to be able to detect the exact number of ongoing transmissions in the network which is difficult to achieve in wireless environment. To ensure proper operation of the protocol the STAs also need to transmit data in such a way that the preambles of multiple packets do not overlap. Thus, the asynchronous transmission protocol is both too complex and incompatible with IEEE 802.11ac protocol.

An uplink MMSE detection based MU-MIMO protocol is proposed in [15] for the IEEE 802.11 WLAN. In this protocol

STAs use OFDMA technique to transmit access request to AP and TDMA technique to transmit pilot signals. However, in IEEE 802.11ac amendment, the training frames are explicitly included in the preamble of the data to determine channel state information which eliminates the need for separate pilot signal transmission during contention period. Markov chain based analytical models for asynchronous MPR techniques are proposed in [16]–[18] but without discussing the underlying MAC protocols. Instead, these proposals focus on the development of theoretical analysis to identify the relevant parameters and the achievable performance.

A multi-user MAC (MU-MAC) that incorporates both multi-packet reception (MPR) and multi-packet transmission by an IEEE 802.11n AP using orthogonal frequency-division multiplexing (OFDM) was described in [19]. However, the protocol does not have any control over the number of RTSs in the uplink: if the number of RTSs exceeds the maximum number of antennas, all packets are lost due to collision and all the STAs involved in collision double the backoff window. The performance of the network will thus be impaired, esp. when it contains a large number of nodes. A multi-round contention based random access MAC protocol for MPR is proposed in [20]. However, the additional contention round leads to higher channel-contention overhead and therefore, there is always a trade-off between channel utilization and contention overhead. A Unified MUMAC (Uni-MUMAC) for IEEE 802.11ac protocol is proposed in [21]. In the uplink transmission the protocol introduces two rounds of contention period. The contention rounds are similar to normal EDCA access technique and unlikely to utilize the full capability of the AP resources. Again multiple RTSs and short inter frame spacing times (SIFS) reduce effective data transmission time and efficiency of the network.

III. Proposed A-MAC Protocol

We assume that our network has only one AP and a number of peripheral STAs in an isolated basic service subsystem (BSS) such that there will be no interference from the nearby BSS. For simplicity, we assume that each STA has only one antenna and the AP has four antennas. To maintain compatibility with the downlink MU-MIMO, we assume that AP can receive four data packets simultaneously from four different STAs. The traffic in AP or STA can be categorized in four priority categories ($k = 0, 1, 2, 3$) in ascending priorities and each category of traffic contends for medium using its own EDCA function. During association with AP, each STA is assigned a block of orthogonal subcarriers for a specified duration. After the expiry of the association duration, the subcarrier block is released and STA initiates reassociation process with the AP during which another block is reassigned to the STA. The size of the subcarrier block is a configuration parameter depending on the density of STAs in the network. For 160 MHz UNII-1 and UNII-2 bands we allocate 5MHz block for each STA so that the network can support a maximum of 32 STAs.

In single user transmission a STA sends an RTS at the end of backoff process. Similarly in a downlink MU transmission, one group RTS is transmitted by the AP to the desired destinations as AP has the knowledge of the destination of packets in its queue. However, in MU uplink transmission AP has no knowledge of the length of the queues of sender nodes. Therefore, during design of A-MAC protocol we have introduced two rounds of RTS transmission. In first round, only the STA that wins the access to the medium through EDCA contention, is allowed to transmit RTS. We denote this STA as the primary STA and the corresponding RTS is named as primary RTS. The primary RTS is duplicated in all 20 MHz channels to ensure backward compatibility with legacy devices. The rest of the nodes in the network are denoted as secondary STAs. The secondary STAs that are in backoff process get opportunities to transmit RTSs to send indications to AP of their intention to transmit packets. These RTSs are denoted as secondary RTSs. Secondary RTS transmission starts after DIFS period of the primary RTS when AP allows MU transmission. The purpose of 5MHz subcarrier allocation during association is to facilitate the channel sounding and transmission of multiple secondary RTSs in OFDMA fashion.

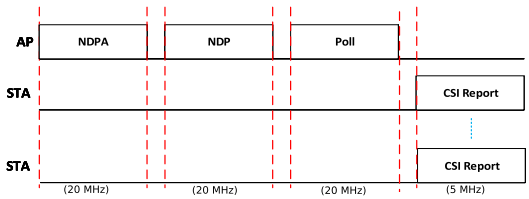

Fig. 1. Channel Sounding by AP.

The successful decoding of concurrent multiple uplink transmission depends on CSI report from STAs. The channel sounding technique in the proposed model is shown in Fig. 1. AP periodically performs channel sounding by sending null data packet (NDP) and in response, STAs transmit the reports using OFDMA technique using the subcarrier blocks assigned during association. The secondary STAs transmit RTSs simultaneously in the second round using previously assigned OFDM subcarrier blocks. These STAs are defined as secondary STAs. Due to unavailability of subcarrier blocks, if the AP is unable to allocate a subcarrier block to a STA, the usual operation is not impacted but the STA cannot participate in the second RTS transmission.

The frame exchange sequence of the proposed protocol is shown in Fig. 2. As soon as the medium becomes idle, all STAs start backoff process. When STA1 wins the contention, STA1 sends RTS. Since the network does not have any hidden terminals and all STAs hear each other, the AP and STAs have the knowledge about the collision of first round RTS. If the collision happens, the primary STA initiates next backoff phase. On hearing RTS, secondary STAs suppress the backoff counting and update the NAV according to the duration information in RTS. Receiving STAs (including AP) decode RTS signal to find the intended destination address. If the RTS is intended for AP and AP decides to allow multi-user transmission, AP defers the transmission of G-CTS up to DIFS period. If AP cannot allow multiple transmission simultaneously, it sends CTS after SIFS period as shown in Fig 3. If primary STA listens CTS after SIFS period, the primary STA starts data transmission after SIFS period

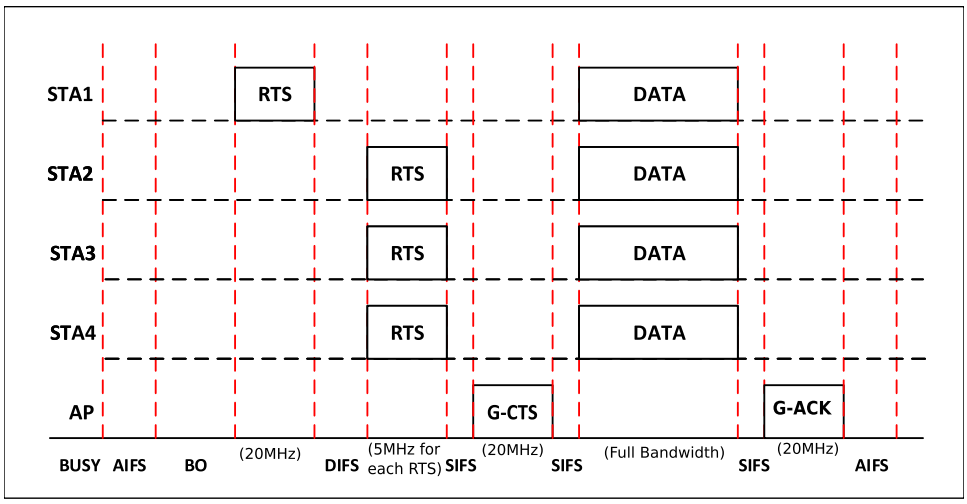

Fig. 2. Multi-STA transmission in A-MAC enabled network.

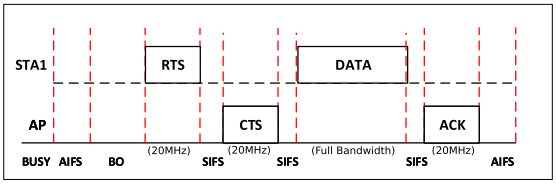

Fig. 3. Single STA transmission

and other STAs keep the backoff countdown suppressed until the medium is idle again. However, if no CTS is transmitted by AP to primary STA after SIFS period, other STAs are allowed to transmit concurrent RTSs using previously allocated OFDM subcarrier blocks. It is fair to assume that AP is connected to the infrastructure and has no capability constrain in monitoring each subcarrier block to retrieve all secondary RTSs. Depending on the number of STAs, it is possible that AP receives larger number of RTSs than the number of antennas M_{ant} in AP.

Based on the CSI report, AP selects a group of up to four STAs including primary STA that are most feasible to transmit data packets simultaneously. AP sends G-CTS to selected STAs using group address. All other STAs update the NAV according to the duration of transmission advertised in G-CTS. The selection algorithm may also vary according to the performance goal such as throughput maximization or fairness consideration. STAs transmit data simultaneously over the whole spectrum for a duration controlled by TXOP duration of STA1. Secondary STAs can transmit up to the duration advertised by AP and in no way can stress the TXOP period of STA1. The STAs can transmit aggregated packets and piggyback the information about the next packet duration. AP can successfully decode all the data using zero forcing (ZF) or minimum mean square error (MMSE) technique extensively used for MPR in WLAN. When the STAs finish transmission or TXOP period expires, AP sends G-ACK to the STAs from which AP receives data successfully. The frame format for G-CTS and G-ACK in our proposed protocol remains the same as CTS and ACK in IEEE 802.11ac protocol. We assume that any combination of STAs in the network can somehow be represented by a group ID so that the destination address in CTS and ACK frames can be replaced by group ID during multiple concurrent transmissions. The duration in G-CTS is set to be the transmission duration of primary STA. The operation of the proposed protocol is shown in Algorithm 1.

Algorithm 1 A-MAC Protocol

Initialization: Packet arrive in STAs, $t = 0$
if *medium == idle* **then**
  if *BO counter != 0* **then**
    STAs decrease BO counter
  else
    STA$_k$ Sends RTS, $t \leftarrow t + waittime + BO$
    STA$_{h \neq k}$ stop BO decrement
else
  wait for medium
if *empty (queue of STA$_{h \neq k}$)* **then**
  AP sends CTS, $t \leftarrow t + SIFS$
  STA$_{h \neq k}$ update NAV
  STA$_k$ transmits data, $t \leftarrow t + SIFS$
else
  AP defers G-CTS
  STA$_{h \neq k}$ transmit RTS, $t \leftarrow t + DIFS$
AP sends G-CTS, $t \leftarrow t + DIFS + SIFS$
STA$_k$ sends data, $t \leftarrow t + SIFS$
if *STA$_{h \neq k}$ in group ID* **then**
  STA$_{h \neq k}$ send data, $t \leftarrow t + SIFS$
else
  STA$_{h \neq k}$ update NAV
  STA$_{h \neq k}$ wait for medium
AP sends G-ACK, $t \leftarrow t + SIFS$
STA$_k$, STA$_{h \neq k}$ receive G-ACK

IV. Analytical Model

We assume that the transmission opportunity of different priority traffic categories in a STA is first resolved through

internal contention using their own EDCA functions. Therefore, each STA contending for medium can be represented by a single priority traffic category. The four different priority STAs in our model are represented by STA_k where $k = 0, 1, 2, 3$ denote priorities in ascending order for Background, Best Effort, Video, and Voice traffic respectively. In normal working environment both AP and STAs contend for the channel at the same time. When AP gains access to the medium, downlink MU-MIMO transmission is initiated and when a STA gains access to the medium, an uplink MU-MIMO transmission is initiated. We have evaluated the performance of DL-MU-MIMO in our previous work [22]. In this paper, we restrict our analysis only for the uplink traffic in order to reduce the complexity of our analytical model. However, we would expect even better network performance in the presence of both uplink and downlink traffic due to the absence of addition control signals in DL-MU-MIMO transmission. Section IV is divided in four sub-sections. In sub-section IV-A we first find the total backoff duration for each traffic category. Sub-section IV-B deals with the queuing model in order to find the state of the queue before and after each transmission. In sub-section IV-C we discuss the Markov chain which models states of STA. Finally, in sub-section IV-D we calculate different performance metrics of the network.

A. Backoff Model

This sub-section has three parts: part IV-A1 determines the probability of transmitting multiple RTSs, part IV-A2 calculates the transmission time for which the backoff counter is suspended and part IV-A1 calculates the total bandwidth reservation time for both successful and unsuccessful transmission.

1) TXOP Sharing Probability: We consider a uniform Poisson packet arrival rate λ_k packets/s for each traffic category. In our analysis the time is slotted and the activity of any node takes place at the edge of a 9μ sec time slot. The duration of A-MPDU, RTS, G-CTS and G-ACK are represented by l_d, rts, cts and ack time slots respectively. The duration of $AIFS_k$, SIFS and DIFS periods are denoted by aifs_k, sifs and difs respectively. We assume a non-ideal channel with bit error rate ber so that there is a probability that the primary RTS and data packets can be corrupt during transmission.

We assume that in our network n_k STAs of class *k* contend for the medium. The total number of contending STAs in the network $N_{\sum} = \sum_{k=0}^{3} n_k$. Each STA has a transmission probability τ_k. Let us assume that AP receives data packets from D_{up} $(1 \leq D_{up} \leq 4)$ STAs simultaneously during MU transmission in uplink. When the number of secondary RTSs are larger than $D_{up} - 1$, AP chooses $D_{up} - 1$ secondary STAs based on selection criteria. In other words, all secondary STAs that send RTSs, may not get the chance to participate in the MU transmission. We first determine the probability of successful transmission of a primary RTS by a particular traffic category k. If only one STA_k is to win the contention and send primary RTS, $n_k - 1$ $STA_k s$ as well as all $STA_{h \neq k}$ must be idle. The probability that a STA_k wins the contention is given by:

$$p_{rts}[k,1] = \tau_k n_k (1-\tau_k)^{n_k - 1} \frac{\prod_{h=0}^{3}(1-\tau_h)^{n_h}}{(1-\tau_k)^{n_k}} \quad (1)$$

where $p_{rts}[k,1]$ is the probability that the primary RTS is sent by k category traffic node. The total probability of transmitting only one primary RTS by all categories is the sum of probabilities of each individual category and is given as:

$$p_{rts}[1] = \sum_{k=0}^{3} p_{rts}[k,1]. \quad (2)$$

The secondary RTSs can be transmitted by all traffic categories depending on the length of the queues of the nodes. If category k has transmitted the primary RTS, then one secondary RTS can be generated either from $n_k - 1$ nodes or from any of the $n_{h \neq k}$ nodes. The probability of transmitting secondary RTS is conditioned on successful transmission of primary RTS. At this point, we define $\pi_{k,0}$ be the probability that the queue of STA_k is empty at the end of TXOP period. The detail expression for $\pi_{k,0}$ will be derived in the subsection (IV-B). When a STA_k transmits primary RTS, one or more secondary RTS/RTSs can be transmitted by any other node/nodes from any other category. However, the transmission of secondary RTS is conditioned on the transmission of primary RTS $p_{rts}[k,1]$. The probability $p_{rts}[t]$ of transmitting *t* $(2 \leq t \leq N_{\sum})$ RTSs (one primary RTS and *t-1* secondary RTSs) *t* can be written as follows:

$$\begin{aligned}
p_{rts}[2] &= \sum_{k=0}^{3}\left[p_{rts}[k,1]\binom{n_k-1}{1}(1-\pi_{k,0})(\pi_{k,0})^{n_k-2}\prod_{h\subset k,h\neq k}\pi_{h,0}^{n_h}\right]\\
p_{rts}[3] &= \sum_{k=0}^{3}\left[p_{rts}[k,1]\binom{n_k-1}{2}(1-\pi_{k,0})^2(\pi_{k,0})^{n_k-3}\prod_{h\subset k,h\neq k}\pi_{h,0}^{n_h}\right]\\
&\quad+\frac{1}{2}\sum_{k=0}^{3}\left[p_{rts}[k,1]\binom{n_k-1}{1}(1-\pi_{k,0})(\pi_{k,0})^{n_k-2}\sum_{h\subset k,h\neq k}\left\{\binom{n_h-1}{1}(1-\pi_{h,0})(\pi_{h,0})^{n_h-1}\prod_{l\subset h,l\neq h}\pi_{l,0}^{n_l}\right\}\right]\\
&\vdots\\
p_{rts}[N_{\sum}] &= \sum_{k=0}^{3}\left[p_{rts}[k,1]\binom{n_k-1}{n_k-1}(1-\pi_{k,0})^{n_k-1}\prod_{h\subset k,h\neq k}\binom{n_h}{n_h}(1-\pi_{h,0})^{n_h}\right] \quad (3)
\end{aligned}$$

where $p_{rts}[n]$ is the probability that a total of n RTSs (primary and secondary) will be transmitted before the start

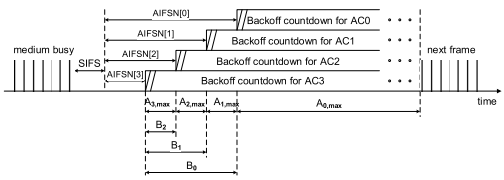

Fig. 4. EDCA channel prioritized access (adopted from [23]).

of MU-TXOP. In equation (2) we see that the transmission of primary RTS from a STA is related to the transmission probability of the particular STA whereas in equation (3), the transmission of secondary RTSs are related to the state of queues of secondary STAs. The Probability Generating Function (PGF) for the number of transmitted RTSs can be written as: $F_{rts}(z) = \sum_{t=0}^{N_\Sigma} p_{rts}[t]z^t$ where $p_{rts}[0]$ is the probability that no node is in the state of transmitting RTS during a time slot. $p_{rts}[0]$ can be expressed as

$$p_{rts}[0] = \prod_{k=0}^{3}(1-\tau_k)^{n_k}. \tag{4}$$

When the number of transmitted RTSs is less than or equal to four, all participating STAs receive G-CTS from the AP; otherwise, only four of the STAs receive G-CTS. Probability $p_{cts}[i]$ that *i* STAs receive G-CTS can be expressed as

$$p_{cts}[i] = \begin{cases} p_{rts}[i], & i = 0\,..\,D_{up}-1 \\ \sum_{t=0}^{N_\Sigma} p_{rts}[t] - \sum_{t=0}^{D_{up}-1} p_{rts}[t], & i = D_{up}. \end{cases} \tag{5}$$

Now the probability $fm[t]$ that a particular secondary STA will be chosen to receive G-CTS from *t* RTSs can be written as

$$fm[t] = \begin{cases} p_{rts}[t+1], & 1 \le t \le D_{up}-1 \\ \dfrac{D_{up}-1}{t-1} p_{rts}[t+1], & D_{up} \le t \le N_\Sigma. \end{cases} \tag{6}$$

Mean probability of receiving G-CTS by a particular secondary STA is given by

$$f_{mu} = \frac{1}{N_\Sigma} \sum_{t=1}^{N_\Sigma} fm[t]. \tag{7}$$

Last equation gives the probability that STA_k will be considered for MU transmission even when the STA is in backoff process. For simplicity of our analysis we assume average value of $fm[t]$ for all STA_k.

EDCA channel access technique for a STA is shown in Fig. 4. The probability f_k that a time slot will be idle during the interval $A_{k,max}$ can be related to the channel access probability τ_k as

$$f_k = \prod_{i=k}^{3}(1-\tau_i)^{n_i}. \tag{8}$$

2) TXOP Duration: During data transmission phase the number of concurrent transmissions depend on the STAs that receive G-CTS from AP. Let $\theta[i]$ be the probability that *i* data packets are transmitted concurrently in a burst during MU uplink transmission. The PGF for the number of data packets in the burst can be obtained as

$$\Theta(z) = \sum_{i=1}^{D_{up}} \theta[i] z^i \tag{9}$$

and the average number of packets in a burst is given by $Mb_k = \Theta'_k(1)$. If $\psi_{k,\mu}$ denotes the probability that μ bursts are transmitted during TXOP period of primary STA, the PGF for the number of bursts transmitted during TXOP is given by $\Phi_k(z) = \sum_{\mu=1}^{M_k} \psi_{k,\mu} \Theta_k(z)^\mu$. The PGF for the duration of a single burst $Tburst_k(z)$ is obtained from Fig. 2 as

$$Tburst_k(z) = z^{l_d + ack + 2sifs} \tag{10}$$

and the average duration (slots) of the burst is $Tburst'_k(1)$. The PGF for total TXOP duration is

$$Ttxop_k(z) = z^{2rts+difs+2sifs+cts+aifs_k} \sum_{\mu=1}^{M_k} \psi_{k,\mu} Tburst_k(z)^\mu \tag{11}$$

with an average duration of $Ttxop'_k(1)$.

3) Duration of Bandwidth Reservation: Successful medium access probability of primary STA during A_l period, as shown in Fig. 4, is given by

$$ps_l = \sum_{i=l}^{3} \frac{n_i \tau_i \prod_{j=l}^{3}(1-\tau_j)^{n_j}}{1-\tau_i}. \tag{12}$$

If secondary STAs are allowed to transmit at a probability f_{mu} during the successful access to the medium by primary STA, the freezing counter restart probability of STA_k $(k < l)$ due to successful transmission is given by

$$psf_l = ps_l(1 - f_{mu}) \tag{13}$$

and freezing counter restart probability of STA_k $(k < l)$ due to unsuccessful reservation of bandwidth is $pff_l = 1 - f_l - ps_l$. However, the backoff counter suppression probability of a STA due to successful or unsuccessful bandwidth reservation during MU-UL transmission remains same as derived in [22].

The PGF for the duration of unsuccessful bandwidth reservation $Tc_k(z)$ due to collision of multiple primary RTSs or the corruption of G-CTS can be obtained as

$$Tc_k(z) = \gamma_k \delta_r (1-\delta_c) z^{2rts+difs+2sifs+cts+Tburst'_k(1)} + \left[1 - \gamma_k \delta_r (1-\delta_c)\right] z^{2rts+difs+2sifs+cts} \tag{14}$$

where γ_k is the probability of successful packet transmission, δ_r is the probability that there will be no RTS error due to noise in the channel and δ_c is the probability that there will be no G-CTS error.

The PGF for the duration of successful access to the medium by all ACs during A_r, $\{r = 0, 1, 2, 3\}$ period can be written

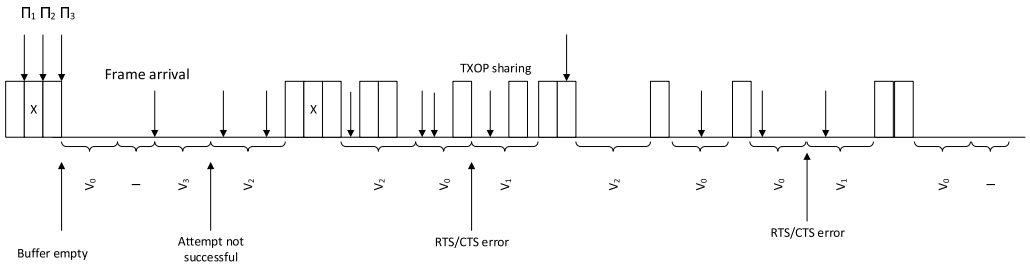

Fig. 5. Timing diagram of the queuing model.

as

$$Ts_r(z) = \frac{\sum_{i=r}^{3} \tau_i n_i Ttxop_r(z)}{\sum_{i=r}^{3} n_i \tau_i}. \quad (15)$$

Finally, the PGFs for backoff time for STA_k during i backoff phase $Tbi_{k,i}(z)$, total backoff time $Tb_k(z)$ and proactive zeroth backoff time $Tb0_k(z)$ can be derived in a similar fashion as discussed in [22].

4) Impact of Hidden Nodes: In our network we assume that AP is located at the center of the BSS and the transmission range of all the nodes are equal. From AP point of view there will be no hidden node since all the nodes within the BSS are associated with the AP and are within the transmission range of AP. Therefore, as soon as AP transmits CTS/G-CTS, all the nodes will update the NAV accordingly so that there will be no collision for data and ACK/G-ACK message. However, when a node (specifically at the periphery of the BSS) transmits RTS, some nodes within the BSS which are outside the transmission range of RTS transmitting node, act as hidden nodes and create collisions. The vulnerable period during which a collision at AP can take place for single user transmission is given as $T_{v-su} = 2.(RTS\_tx\_time + SIFS + CTS\_tx\_time)$. Similarly, the vulnerable period for MU transmission is given as:$T_{v-mu} = 2.(2.RTS\_tx\_time + DIFS + SIFS + CTS\_tx\_time)$. Let $N_{k,h}$ be the number of hidden nodes of traffic category k for a transmitting node. The probability f_h that a hidden node will not transmit in a time slot during vulnerable period T_{v-mu} can be written as

$$f_h = \sum_{k=0}^{3} \frac{(1-\tau_k)^{N_{k,h}}}{\tau_k N_{k,h}} \quad (16)$$

The probability f_{ncoll} that there will be no collision from the hidden nodes during the entire vulnerable period is given as

$$f_{ncoll} = f_h^{(1-f_{mu})T_{v-su}+f_{mu}T_{v-mu}} \quad (17)$$

where f_{mu} is the MU transmission probability defined in (7). Now, the successful transmission probability in presence of hidden nodes $\gamma_{k,h}$ can be evaluated as $\gamma_{k,h} = \gamma_k f_{ncoll}$ where γ_k is the successful transmission probability without hidden node [22].

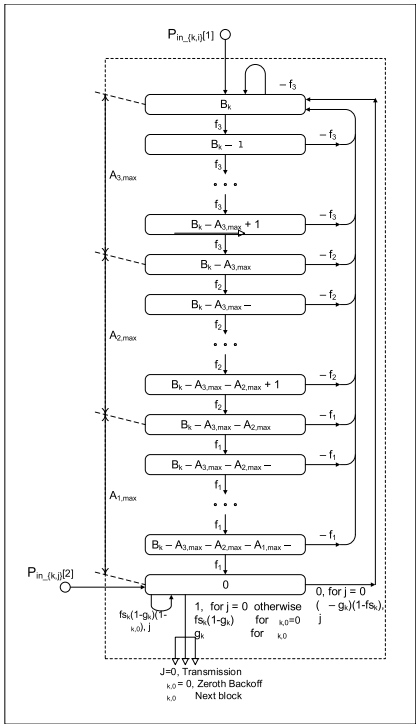

Fig. 6. Basic block of the Markov chain model, adapted from [23].

B. Queuing Model

The state of the queue of STA_k before the start of TXOP period and after the transmission of a packet is represented by the timing diagram shown in Fig. 5 and the Markov chain model shown in Fig. 7. Now we will develop the equation for the probability for i packets in the queue of a STA. Let STA_k has just finished the transmission and $\pi_{k,0}^{(\mu)}$ be the probability that queue of STA_k is empty after the transmission of μ packets. STA_k will go through proactive zeroth backoff process. During proactive zeroth backoff process let $v_{k,0}^0$ be the probability that zero packet arrive during v^0 period. If there is no packet arrival at the end of proactive zeroth backoff state, STA_k goes to idle state and remains idle until a packet arrives. STA_k will sense the medium and if the medium is idle for a period of AIFS_k which we denote by v^3, STA_k will start transmission at the end of v^3 period. The probability that the medium will be idle for a period of AIFS_k is $f_0^{aifs_k}$. Now in order to have i packets in the queue before the start of transmission we need $i-1$ packet arrival during v^3 period. When all

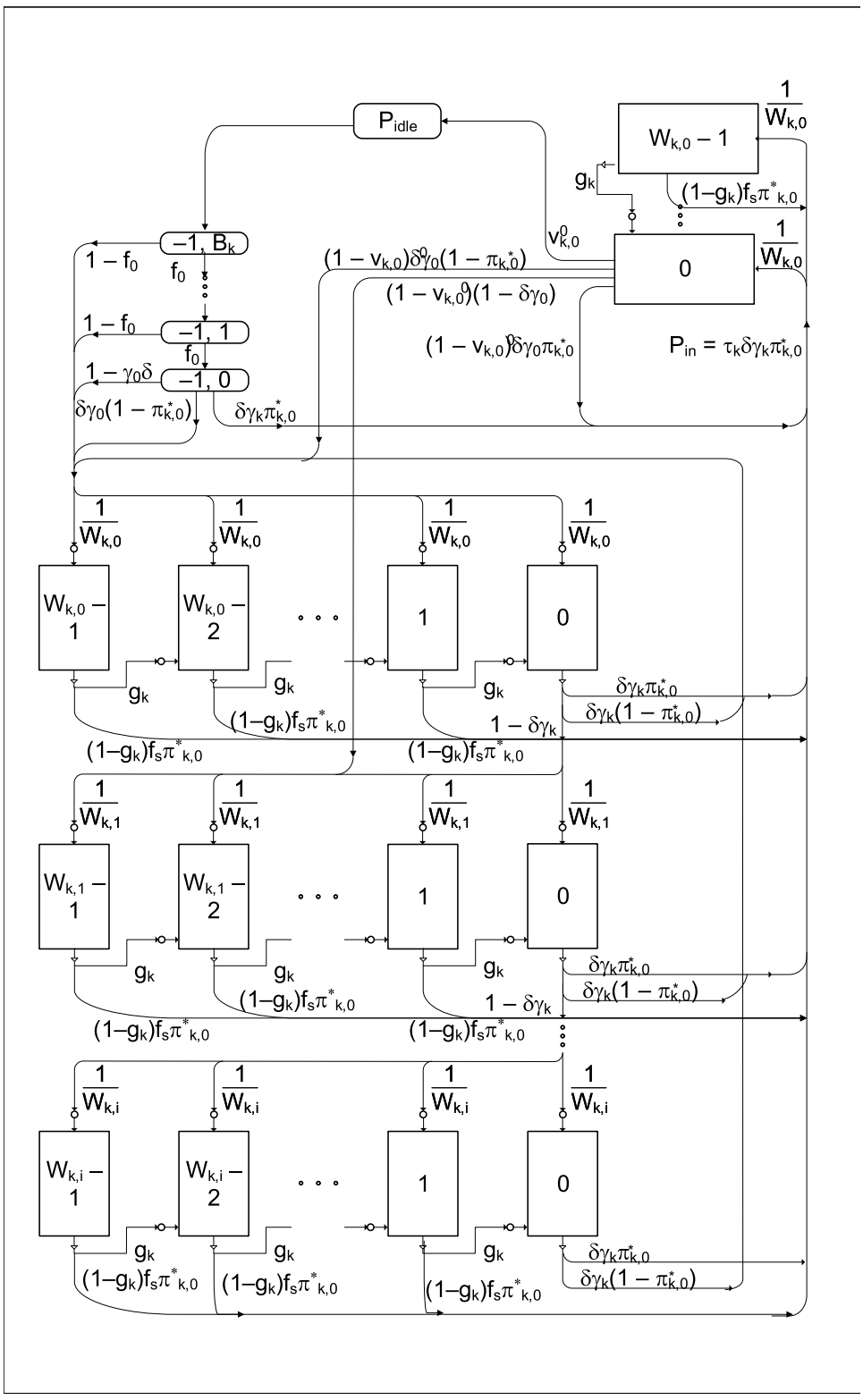

Fig. 7. Markov Chain for STA$_k$.

the above conditions are met, the first term of the equation can be written as $f_0^{aifs_k} v_{k,0}^0 \sum_{\mu=1}^{M_k} \pi_{k,0}^{(\mu)} v_{k,i-1}^3$. During v^3 period STA$_k$ will not participate in MU transmission as secondary STA. $(1 - f_0^{aifs_k})$ is the probability that the medium will be busy during v^3 period. The STA$_k$ will start full backoff process and the duration of full backoff process is denoted by v^2. During v^2 backoff period STA_k can participate in transmission as secondary STA or start transmission as primary STA at the end of v^2 period. The second and third terms can be written based on these conditions. Similarly we can include all the transmission scenarios and the probabilities are summed up to find the total probability of having i packets

in the queue before the start of transmission. The complete equation is written as follows:

$$
\begin{aligned}
&q^{+}_{k,i}(z)\\
&= f_0^{aifs_k} v^0_{k,0} \sum_{\mu=1}^{M_k} \pi^{(\mu)}_{k,0} v^3_{k,i-1}\\
&\quad +(1-f_0^{aifs_k})(1-f_{mu})^2 v^0_{k,0} \sum_{\mu=1}^{M_k} \pi^{(\mu)}_{k,0} \sum_{j=0}^{i-1} v^3_{k,j} v^2_{k,i-j}\\
&\quad + f_{mu}(1-f_0^{aifs_k})(1-f_{mu}) v^0_{k,0} \sum_{\mu=1}^{M_k} \pi^{(\mu)}_{k,0} \sum_{j=0}^{i-1} v^3_{k,j} v^{2+}_{k,i-j}\\
&\quad + (1-f_0^{aifs_k}) f_{mu}(1-f_{mu}) v^0_{k,0} \sum_{\mu=1}^{M_a} \pi^{(\mu)}_{k,0} \sum_{j=0}^{i-1} v^3_{k,j} v^2_{k,i-j}\\
&\quad + (1-f_0^{aifs_k}) f^2_{mu} v^0_{k,0} \sum_{\mu=1}^{M_a} \pi^{(\mu)}_{k,0} \sum_{j=0}^{i-1} v^3_{k,j} v^{2+}_{k,i-j}\\
&\quad + f_{mu}(1-f_{mu}) \sum_{\mu=1}^{M_k} \pi^{(\mu)}_{k,0} v^{0+}_{k,i} + f^2_{mu} \sum_{\mu=1}^{M_a} \pi^{(\mu)}_{k,0} v^{0+}_{k,i}\\
&\quad + (1-f_{mu}) \sum_{\mu=1}^{M_k} \pi^{(\mu)}_{k,0} v^0_{k,i} \gamma_k \delta\\
&\quad + (1-f_{mu})^3 (1-\gamma_k\delta) \sum_{\mu=1}^{M_k} \pi^{(\mu)}_{k,0} \sum_{j=1}^{i} v^0_{k,i} v^1_{k,i-j}\\
&\quad + f_{mu}(1-f_{mu})^2 (1-\gamma_k\delta) \sum_{\mu=1}^{M_k} \pi^{(\mu)}_{k,0} \sum_{j=1}^{i} v^0_{k,i} v^{1+}_{k,i-j}\\
&\quad + f_{mu}(1-f_{mu})^2 (1-\gamma_k\delta) \sum_{\mu=1}^{M_a} \pi^{(\mu)}_{k,0} \sum_{j=1}^{i} v^0_{k,i} v^1_{k,i-j}\\
&\quad + f^2_{mu}(1-f_{mu})(1-\gamma_k\delta) \sum_{\mu=1}^{M_a} \pi^{(\mu)}_{k,0} \sum_{j=1}^{i} v^0_{k,i} v^{1+}_{k,i-j}\\
&\quad + (1-f_{mu}) \sum_{j=1}^{i} \pi^{M_k}_{k,j} \left[(1-f_{mu}) v^2_{k,i-j} + f_{mu} v^{2+}_{k,i-j} \right]\\
&\quad + f_{mu}\gamma_k\delta \sum_{j=1}^{i} \pi^{M_a}_{k,j} v^{0+}_{k,i-j}\\
&\quad + f_{mu}(1-f_{mu})(1-\gamma_k\delta) \sum_{j=1}^{i} \pi^{M_a}_{k,j} \sum_{l=0}^{i-j} v^{0+}_{k,l} v^1_{k,i-j-l}\\
&\quad + f^2_{mu}(1-\gamma_k\delta) \sum_{j=1}^{i} \pi^{M_a}_{k,j} \sum_{l=0}^{i-j} v^{0+}_{k,l} v^{1+}_{k,i-j-l}. \qquad (18)
\end{aligned}
$$

f_{mu} is the probability that STA$_k$ will participate in transmission of MU uplink as secondary STA which we have defined in equation(7). M_k and $M_{a\subset k}$ are the number of packets transmitted by STA$_k$ as primary STA and secondary STA respectively. v^0, v^1, v^2 and v^3 are the probabilities for the duration of zeroth backoff, full backoff without zeroth backoff, full backoff and idle period respectively as shown in Fig. 5. v^{0+}, v^{1+} and v^{2+} are the probabilities of residual backoff time for the corresponding region. The terms associated with $(1-f_{mu})$ are the state of queue when the STA participates in the transmission as primary STA and the terms associated with f_{mu} are the state of queue when STA participate in MU transmission as secondary STA. The product $\gamma_k\delta$ is the probability that the transmission is successful. To find a closed form solution of the equation we assume $M_a = M_k$ which means STA$_k$ transmits M_k packets in both primary and secondary transmissions. When STA$_k$ transmits packet as secondary STA, M_a depends on the traffic category of primary STA. So our assumption leads to a specific case when both the primary STA and the secondary STA are of same priority category. After summation and simplification we find the PGF for the queue length $Q^+_k(z) = \sum_{i=1}^{\infty} q^+_{k,i}$ where the numerator and denominator are given by

$$
\begin{aligned}
&num(Q^+_k(z))\\
&\quad = z^{M_k+1} f_0^{aifs_k} v^0_{k,0} F_{k,3}(z) \sum_{\mu=1}^{M_k} \pi^{(\mu)}_{k,0}\\
&\qquad + z^{M_k+1}(1-f_0^{aifs_k}) v^0_{k,0} F_{k,3}(z) \sum_{\mu=1}^{M_k} \pi^{(\mu)}_{k,0}\\
&\qquad \times \left[(1-f_{mu}) F_{k,2}(z) + f_{mu} F^+_{k,2}(z) \right]\\
&\qquad + \left[f_{mu} + (1-f_{mu})\gamma_k\delta \right] \left[F^+_{k,0}(z) - v^0_{k,0} \right]\\
&\qquad \times \sum_{\mu=1}^{M_k} \pi^{(\mu)}_{k,0} + (1-f_{mu})^2 (1-\gamma_k\delta) \left[F^+_{k,0} - v^0_{k,0} \right]\\
&\qquad \times F_{k,1}(z) \sum_{\mu=1}^{M_k} \pi^{(\mu)}_{k,0} + f_{mu}(1-f_{mu})(1-\gamma_k\delta)\\
&\qquad \times \left[F^+_{k,0} - v^0_{k,0} \right] F^+_{k,1}(z) \sum_{\mu=1}^{M_k} \pi^{(\mu)}_{k,0}\\
&\qquad - (1-f_{mu})^2 F_{k,2}(z) \sum_{\mu=1}^{M_k} \pi^{(\mu)}_{k,0} \Omega_K(z)^{M_k-\mu}\\
&\qquad - f_{mu}(1-f_{mu}) F^+_{k,2}(z) \sum_{\mu=1}^{M_k} \pi^{(\mu)}_{k,0} \Omega_K(z)^{M_k-\mu}\\
&\qquad - f_{mu}\gamma_k\delta F^+_{k,0}(z) \sum_{\mu=1}^{M_k} \pi^{(\mu)}_{k,0} \Omega_K(z)^{M_k-\mu}\\
&\qquad - f_{mu}(1-f_{mu})(1-\gamma_k\delta) F^+_{k,0}(z) F_{k,1}(z)\\
&\qquad \times \sum_{\mu=1}^{M_k} \pi^{(\mu)}_{k,0} \Omega_K(z)^{M_k-\mu} - f^2_{mu}(1-\gamma_k\delta)\\
&\qquad \times F^+_{k,0}(z) F^+_{k,1}(z) \sum_{\mu=1}^{M_k} \pi^{(\mu)}_{k,0} \Omega_K(z)^{M_k-\mu} \qquad (19)
\end{aligned}
$$

and

$$
\begin{aligned}
&den(Q^+_k(z))\\
&= z^{M_k} - \Big[(1-f_{mu}) F_{k,2}(z) + f_{mu} F^+_{k,2}(z)\\
&\qquad + f_{mu}\gamma_k\delta F^+_{k,0}(z) + f_{mu}(1-f_{mu})(1-\gamma_k\delta)\\
&\qquad \times F^+_{k,0}(z) F_{k,1}(z) + f^2_{mu}(1-\gamma_k\delta) F^+_{k,0}(z) F^+_{k,1}(z) \Big]\\
&\quad \times \{ z\Omega_K(z) \}^{M_k} \qquad (20)
\end{aligned}
$$

respectively.

The PGF for the number of frames in the queue after the departure of π-th frame can be written as $\Pi_{k,\mu}(z)$ and is obtained from [22].

Since function $Q_k^+(z)$ is analytical in the range $|z| < 1$, the zeros of the polynomials in the numerator and denominator must be identical. Obviously $z = 1$ is one of the M_k roots of the denominator and the remaining $M_k - 1$ roots can be obtained by using Lagrange's theorem [24]. The sum of the probabilities of the system states before the beginning of TXOP and after the transmission of each packet within TXOP period must be equal to one and therefore, the last equation is obtained from the condition of total probability as

$$(M_k+1)Q_k^+(1) - \sum_{\mu=1}^{M_k-1} \pi_{k,0}^{(\mu)}(M_k-\mu) = 1 \tag{21}$$

which can be expanded and rearranged to read

$$\begin{aligned} M_k(1-\rho_k') - Fac_k'(1) &= (M_k+1)num(Q_k^+(1)) \\ &\quad - den(Q_k^+(1)) \sum_{\mu=1}^{M_k} \pi_{k,0}^{(\mu)}(M_k-\mu) \end{aligned} \tag{22}$$

where

$$\begin{aligned} Fac_k'(1) = {} & (1-f_{mu})^2 F_{k,2}'(1) + f_{mu}(1-f_{mu})F_{k,2}^{+'}(1) \\ & + f_{mu}\gamma_k\delta F_{k,0}^{+'}(1) \\ & + f_{mu}(1-f_{mu})(1-\gamma_k\delta)\left[F_{k,0}^{+'}(1) + F_{k,1}'(1)\right] \\ & + f_{mu}^2(1-\gamma_k\delta)\left[F_{k,0}^{+'}(1) + F_{k,1}^{+'}(1)\right]. \end{aligned}$$

The mean arrival rate during service period is the offered load ρ_k, and $\rho_k' = \rho_k + (1-\sigma)$ is the scaled offered load which takes into consideration the transmission failure. Now M_k equations from (19), (20) and (22) can be solved to obtain the values of M_k unknown variables $\pi_{k,0}^{(M_k)}$.

C. Markov Chain Model

The states of Markov chain model is shown in Fig. 7 where each rectangle represents a basic block as shown in Fig. 6. The bottom three rows of Fig. 7 are the regular backoff phases of a STA and the remaining top portion of the figure represents the proactive zeroth backoff phase. A freezing countdown state which is not shown here due to limitation of space, is associated with each backoff state . Each state in Markov chain is represented as $b_{k,i,j,l}$ where *i* ($0 \le i \le R$) is the backoff phase, *j* ($0 \le j \le W_{k,i} - 1$) is the backoff counter value and *l* ($0 \le l \le B_k$) is the freezing counter value. After successful transmission of packet, STA$_k$ goes to proactive zeroth backoff state when the queue becomes empty. If no packet arrives during proactive zeroth phase, STA goes to idle state. Any packet arrival during proactive zeroth backoff phase initiates a transmission attempt at the end of proactive zeroth backoff phase. After successful transmission of packets if the queue is not empty, STA starts regular backoff process. During backoff process a STA may participate in MU transmission as secondary STA. The input probability to the vertical zeroth backoff stage of the Markov chain model is given as

$$Pin_{k,-2}[1] = \frac{\left[(1-f_{mu})\tau_k\gamma_k\delta + f_{mu}(1-g_k)\gamma_k\delta\right]\pi_{k,0}^*}{W_{k,0}} \tag{23}$$

where $\pi_{k,0}^* = \frac{1}{\Pi_{k,tot}(1)} \sum_{\mu=1}^{M_k} \pi_{k,0}^{(\mu)}$. The first component of the last equation accounts for the situation when STA$_k$ transmits packet as primary STA, while the second quantifies the impact of UL- MU transmission when STA$_k$ gets the opportunity to transmit packet as secondary STA.

The sum of probabilities of all states in the proactive zeroth backoff phase can written as

$$\begin{aligned} S_{k,-2} = {} & Pin_{k,-2}[1]Fnl_k + Pin_{k,-2}[1]\sum_{j=1}^{W_{k,0}-1}\left(\frac{g_k}{y}\right)^j \\ & + Pin_{k,-2}[1]Fl_k\left[W_{k,0}-1\right] \\ & + r_k Pin_{k,-2}[1]Fl_k\sum_{n=1}^{W_{k,0}-2}(W_{k,0}-1-n)\left(\frac{g_k}{y}\right)^n \\ & + \frac{Pin_{k,-2}[1]}{x}\sum_{n=1}^{W_{k,0}-2}(W_{k,0}-1-n)\left(\frac{g_k}{y}\right)^n \end{aligned} \tag{24}$$

where $r_k = \frac{(1-g_k)(1-f_{mu})}{1-f_{mu}(1-g_k)(1-\pi_{k,0})}$, $x = 1 - f_{mu}(1-g_k)(1-\pi_{k,0})$ and $y = (1-r_k)\{1-f_{mu}(1-g_k)(1-\pi_{k,0})\}$. Fl_k and Fnl_k in equation (24) are the factors for loopback and no loopback respectively from the bottom state of basic block of Markov chain during freezing countdown process as defined in [22].

The input probability to the idle state of the Markov chain can be defined as

$$Pin_{k,-1}[1] = v_{k,0}^0 Pin_{k,-2}[1]W_{k,0} \tag{25}$$

and the sum of all probabilities in the idle states of Markov chain can be obtained as

$$S_{k,-1} = Pin_{k,-1}[1]\sum_{i=0}^{aifs_k} f_0^i. \tag{26}$$

The input probability to the horizontal zero-th backoff state is given as

$$\begin{aligned} Pin_{k,0}[1] = {} & \Big[Pin_{k,-1}[1](1-f_0^{aifs_k}) \\ & + Pin_{k,-2}[1](1-v_{k,0}^0)(1-\pi_{k,0}^*)W_{k,0} \\ & + (1-f_{mu})\tau_k\gamma_k\delta(1-\pi_{k,0}^*)\Big]\frac{1}{W_{k,0}}. \end{aligned} \tag{27}$$

The first component of equation (27) accounts for the case when the medium is sensed busy by STA$_k$ during freezing countdown after exiting the idle state. The second term considers the case when STA$_k$ starts transmission at the end of proactive zeroth backoff but the queue is not empty after the TXOP period. At the end of regular backoff process, STA$_k$ starts TXOP period and if the queue of the primary STA is not empty at the end of TXOP period, Primary STA goes to full backoff process whereas the secondary STA resumes backoff countdown from the point where it was considered for UL- MU transmission. This situation is accounted for in the

third term of equation (27). The input probability to the *i*-th state of the Markov chain model is given as:

$$\begin{aligned} &Pin_{k,i}[1] \\ &= \frac{Pin_{k,0}[1]}{\prod_{j=1}^{i} W_{k,j}}(1-\gamma_k\delta)^i \prod_{j=0}^{i-1}\sum_{l=0}^{W_{k,j}-1}(\frac{g_k}{y})^l \\ &\quad + \frac{Pin_{k,-2}[1]W_{k,0}(1-\gamma_k\delta)^i(1-v_{k,0}^0)}{\prod_{j=1}^{i} W_{k,j}} \prod_{j=1}^{i-1}\sum_{l=0}^{W_{k,j}-1}(\frac{g_k}{y})^l. \end{aligned} \tag{28}$$

Finally, the sum of the probabilities of all states in backoff phase *i* can be expressed as:

$$\begin{aligned} S_{k,i} = \Bigg[& Fnl_k + \sum_{n=1}^{W_{k,i}-1}(\frac{g_k}{y})^n + (W_{k,i}-1)Fl_k \\ & + (r_kFl_k + \frac{1}{x})\sum_{n=1}^{W_{k,i}-2}(W_{k,i}-1-n)(\frac{g_k}{y})^n \Bigg] Pin_{k,i}[1]. \end{aligned} \tag{29}$$

Since the probabilities of all states of Markov chain are known, the transmission probability of STA_k can be obtained as:

$$\begin{aligned} \tau_k = {} & b_{k,-2,0,0} + b_{k,-1,0,0} + \sum_{i=0}^{R} b_{k,i,0,0} \\ & + f_{mu}(1-g_k)\left[\sum_{j=1}^{W_{k,0}-1} b_{k,-2,j,0} + \sum_{j=1}^{W_{k,i}-1} b_{k,i,j,0}\right] \end{aligned} \tag{30}$$

in which the first two terms result from the proactive zeroth backoff phase, the third term is the transmission probability when STA_k transmits as primary STA at the end of regular backoff phase and the last term is the increase in transmission probability due to MU-UL transmission when STA_k acts as secondary STA.

D. Throughput Calculation

Laplace-Stieltjes transform (LST) of the time between two consecutive accesses to the network by STA_k can be obtained from the timing diagram shown in Fig.5 as

$$\begin{aligned} &Tcon_k^*(s) \\ &= \Bigg[v_{k,0}^0 f_0^{aifs_k}\pi_{k,0}^* \frac{\lambda_k}{\lambda_k+s} B_{k,0}^*(s)B_{k,3}^*(s) \\ &\quad + v_{k,0}^0(1-f_0^{aifs_k})\pi_{k,0}^* \frac{\lambda_k}{\lambda_k+s} B_{k,0}^*(s)B_{k,3}^*(s) \\ &\quad \times \left\{(1-f_{mu})B_{k,2}^*(s) + f_{mu}B_{k,2}^{+*}(s)\right\} \\ &\quad + (1-v_{k,0}^0)\pi_{k,0}^* \Bigg\{ f_{mu}B_{k,0}^{+*}(s) + (1-f_{mu}) \\ &\quad \times \Big\{\gamma_k\delta B_{k,0}^*(s) + (1-\gamma_k\delta)B_{k,0}^*(s)\Big\{(1-f_{mu}) \\ &\quad \times B_{k,1}^*(s) + f_{mu}B_{k,1}^{+*}(s)\Big\}\Big\}\Bigg\} + (1-\pi_{k,0}^*) \\ &\quad \left\{(1-f_{mu})B_{k,2}^*(s) + f_{mu}B_{k,2}^{+*}(s)\right\}\Bigg] Ttxop_k(e^{-s}) \end{aligned} \tag{31}$$

where $B_{k,0}^*(s)$, $B_{k,1}^*(s)$, and $B_{k,2}^*(s)$ are the LSTs of proactive zeroth backoff time, backoff time excluding zeroth backoff, and full backoff time, respectively. $B_{k,0}^{*+}(s)$, $B_{k,1}^{*+}(s)$, and $B_{k,2}^{*+}(s)$ are the LSTs of the corresponding residual backoff times, and $\frac{\lambda_k}{\lambda_k+s}$ is the LST of residual frame inter-arrival time. If there is no packet arrival during proactive zeroth backoff, STA_k enters into idle state and waits for the elapsed inter arrival time $\frac{\lambda_k}{\lambda_k+s}$. From equation (31), we obtain active duration $Tact_k$ between two consecutive accesses by taking away elapsed inter arrival time.

The PGF for the number of bursts transmitted during TXOP service period can be calculated as

$$\Psi_k(z) = \frac{\sum_{\mu=1}^{M_k-1}\pi_{k,0}^{(\mu)} z^{\mu+M_k}\left(\Pi_{k,tot}(1) - \sum_{\mu=1}^{M_k-1}\pi_{k,0}^{(\mu)}\right)}{\Pi_{k,tot}(1)} \tag{32}$$

where $\Pi_{k,tot}(z) = \sum_{\mu=0}^{M_k}\Pi_{k,\mu}(z)$.

Finally, the average throughput of a STA_k can be calculated as

$$Th_k = \frac{1}{n_k}\frac{Mb_kL_d\overline{\Psi_k(z)}}{\overline{Tcon_k}} \tag{33}$$

where $\overline{Tcon_k}$ is the mean time between two successive accesses to the medium. The cumulative network throughput Th_{net} is given by

$$Th_{net} = \sum_{k=0}^{3} n_kTh_k. \tag{34}$$

We define capacity of the network C_{net} as the traffic intensity at onset of saturation:

$$C_{net} = \sum_{k=0}^{3} n_k\lambda_k \tag{35}$$

where we have defined the onset of saturation as an aggregate packet arrival rate when the average queue size of the lowest priority traffic category becomes two before start of TXOP period. We also define network efficiency η as the ratio of network throughput and traffic intensity as

$$\eta = \frac{Th_{net}}{L_d\sum_{k=0}^{3} n_k\lambda_k} \tag{36}$$

where L_d is the length of data packet.

V. Numerical Results and Discussion

We have used MapleSoft computing software to solve equations (1-20) through iterative approach. The equations in Markov chain model is then evaluated using the obtained solution to generate seeds for next iteration. After a number of iterations, we obtain a stable solution for τ, f, γ and ψ. Using these parameters, we calculate the network metrics. Since all packets are destined to AP, we assume that packet aggregation takes place before placing the MSDU in the queue for scheduling so that we can associate only one queue to each STA. We assume that our VHT PPDU has one MPDU which contains an A-MSDU from LLC layer.

TABLE III
PARAMETERS USED FOR PERFORMANCE EVALUATION OF A-MAC

Parameters	Numerical values	Parameters	Numerical values
Bit error rate, BER	$2 * 10^{-6}$ bits/s	Duration of Time slot, σ	9 μs
Minimum PHY header	40 μs	Maximum PHY header	52 μs
DCF Inter-frame space duration, DIFS	$34\mu s$	MPDU length	11454
Short Inter-frame space duration, SIFS	$16\mu s$	MAC header length	36 bytes
Request to send, RTS	20 bytes	Clear to send, G-CTS	14 bytes
Acknowledgement, G-ACK	32 bytes	Maximum retry limit , R	7
Max. number of antennas in AP, M_{ant}	4	Number of antennas in STA	1
Bandwidth	80 MHz	OFDM symbol duration	4 μs
Number of bits per OFDM symbol duration	1560	Modulation and Coding scheme, MCS	9
Maximum backoff stages	$[5, 5, 1, 1]$	Arbitration inter frame space, AIFS	$[7, 5, 3, 2]$
Minimum contention window size CW_{min}	$[32, 32, 16, 8]$	TXOP duration limit	$[0, 0, 1504, 1504]\mu s$

While evaluating performance metrics for varying number of nodes and packet arrival rates, we first vary number of nodes uniformly and then keeping the number of nodes fixed, we vary packet arrival rates uniformly for all nodes. However, when we evaluate the impact of non uniform packet arrival rate for the nodes, we keep the number of nodes constant for all categories ($N_{\sum} = 24$) and then non-uniformly vary the packet arrival rates for different priority categories. We observe that the patterns of the performance metrics are similar for AC_0 and AC_1 and so we have grouped them as low priority traffic group (LPG). Similarly, AC_2 and AC_3 are grouped as high priority traffic group (HPG). The parameters for the model are shown in Table III.

The analytical model is scalable for up to 32 nodes and any packet arrival rate. The limitation of the number of nodes is imposed by available 5MHz subcarrier blocks. The degree of freedom of polynomials in the model linearly increases with the increase of the number of nodes. This puts extra burden on computing software and memory resources. A feasible solution of the analytical model for a given number of nodes is achieved for a range of packet arrival rates beyond which the system becomes unstable and no real solution is possible. In Figs. (9-11) the notations k_0, k_1, k_2 and k_3 denote traffic priority categories in ascending order, while notations H, E and L correspond to higher intensity of high priority traffic, equal intensity traffic and higher intensity of low priority traffic, respectively.

The average backoff time for different priority groups under uniformly varying load conditions for A-MAC (MU) and 802.11ac (SU) protocol are shown in blue and red, respectively, in Fig. 8. We observe that the average backoff times for all traffic categories are reduced by almost 50% due to concurrent transmission opportunities for STAs. We also observe that MU transmission can sustain higher packet arrival rates than the SU transmission. When number of nodes in each traffic category $n_k = 6$, the system is at onset of saturation at packet arrival rate of $\lambda_k = 50$ packets/s for MU transmission. For SU transmission, the system is at onset of saturation at a much lower packet arrival rate of $\lambda_k = 25$. Fig. 8 shows that with the increase of the number of nodes or packet arrival rate, the backoff time of the STA increases as a STA needs to wait for a longer period to gain access to the medium. It is obvious from Fig. 8 that the low priority traffic group drives the system to saturation point. The average backoff time for low priority

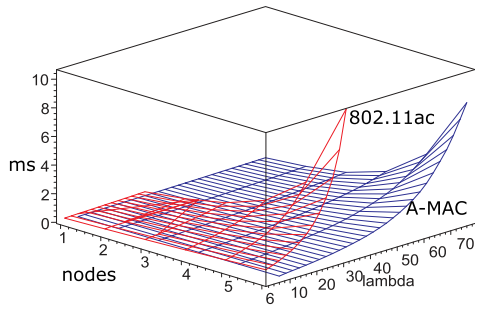

(a) Backoff time of low priority traffic group

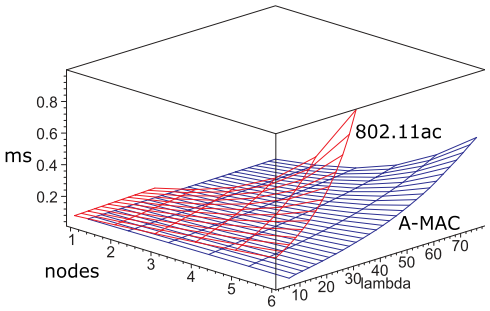

(b) Backoff time of high priority traffic group

Fig. 8. Comparison of backoff time between A-MAC and 802.11ac in uniform traffic condition.

traffic group goes to ten ms at onset of saturation. On the other hand, the backoff time for high priority traffic group remains around tenths of a ms even at high load condition due to smaller AIFS times and smaller contention window size.

For non-uniformly varying packet arrival, Fig. 9(a) shows that when the intensity of higher priority traffic is high, backoff time for lower priority traffic becomes very high (10 ms) at onset of saturation since the network is always busy in serving higher priority traffic and the lower priority traffic has lower opportunity to transmit packets. The backoff time of lower priority traffic decreases to about 4ms as a balance between the higher and lower priority traffic is achieved as shown in Fig. 9(b). The backoff time improves even further to about 2.5ms when the intensity of lower priority traffic exceeds that of the higher priority traffic, Fig. 9(c).

Fig. 10 shows the medium access probability τ_k for different priority STAs. As the load increases, the STAs access the

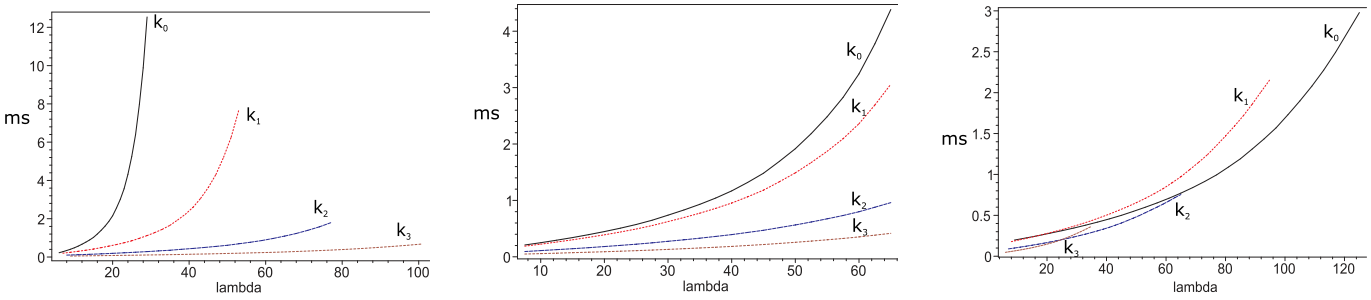

(a) Dominant high priority traffic (b) Equal intensity traffic (c) Dominant low priority traffic

Fig. 9. Backoff time of A-MAC in varying traffic conditions ($N_{\sum} = 24$).

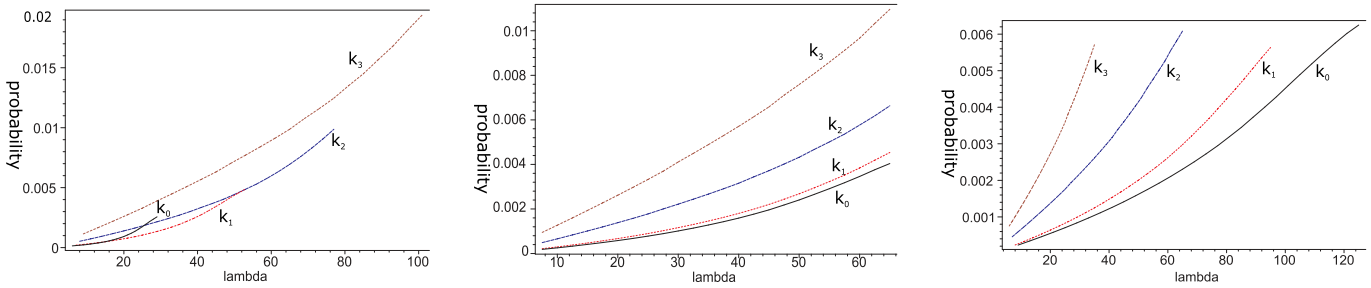

(a) Dominant high priority traffic (b) Equal intensity traffic (c) Dominant low priority traffic

Fig. 10. Medium access probability of a STA (τ_k)($N_{\sum} = 24$).

medium more frequently. As a result, the medium access probability gradually increases with the increase in packet arrival rate of the STA. When the intensity of higher priority traffic is higher than the intensity of lower priority traffic, low priority traffic has less opportunity to access the medium as shown in Fig. 10(a). As the packet arrival rates among different priority categories become balanced, medium access probabilities uniformly increase and when the low priority traffic categories dominate in the network, all categories achieve almost same medium access probability at onset of saturation as shown in Fig. 10(c). Therefore, to ensure fairness among traffic categories, it is desirable to have higher intensity of low priority traffic in the network.

Figs. 11(a)-11(c) show the payload throughput for different traffic categories under non-uniformly varying traffic conditions. In all scenarios, the throughput of high priority traffic group increases almost linearly with the increase in traffic intensity. However, the throughput of low priority group starts declining at higher traffic intensity due to lower transmission opportunity.

From Fig. 11(d) we observe that the network throughput increases with the increase of the number of nodes and packet arrival rates, with the latter having more pronounced impact. At uniformly varying packet arrival rates for all traffic categories, the network throughput steadily increases with the increase of traffic intensity up to the onset of saturation as shown in Fig. 11(d). However, the throughput of low priority traffic decreases drastically at higher traffic intensity and the throughput gain of high priority group is offset by the throughput reduction of low priority traffic group. As a result, overall network throughput decreases. Fig. 11(e) shows a comparison of analytical network throughput between 802.11ac protocol and A-MAC protocol under non-uniformly varying load conditions. We observe that A-MAC throughput is 150% higher than the corresponding 802.11ac throughput. The highest throughput, up to around 5000 packets/s at the onset of saturation, is achieved when the high priority traffic has higher intensity than the low priority one. As the intensity of the low priority traffic increases, throughput falls and we observe a 12.5%drop in throughput when the network has higher intensity of low priority traffic. However, the packet handling capacity of the network at the onset of saturation increases by 40%. Fig. 11(f) shows a comparison of network efficiency which decreases with the increase in traffic intensity due to increasing RTS collisions, retransmission and increased backoff time. Fig. 11(f) also demonstrates that during A-MAC transmission, network efficiency goes as high as 93% due to enhanced network throughput for concurrent multiple uplink transmissions. The efficiency of 802.11ac protocol is lower than A-MAC protocol and it decreases sharply with the increase of offered load.

To verify the proposed analytical model, we have developed an event-based simulator in Matlab environment to simulate the MAC layer of IEEE 802.11ac protocol as well as our proposed protocol. In our simulation we have randomly placed 24 nodes with uniformly varying load intensity for all traffic categories in a $10m \times 10m$ space, with the AP placed at the center. Each simulation is run for 20 seconds and the performance metrics are averaged over 10 runs.

The comparison of simulation results of some important network metrics are shown in Fig. 12, with analytical results

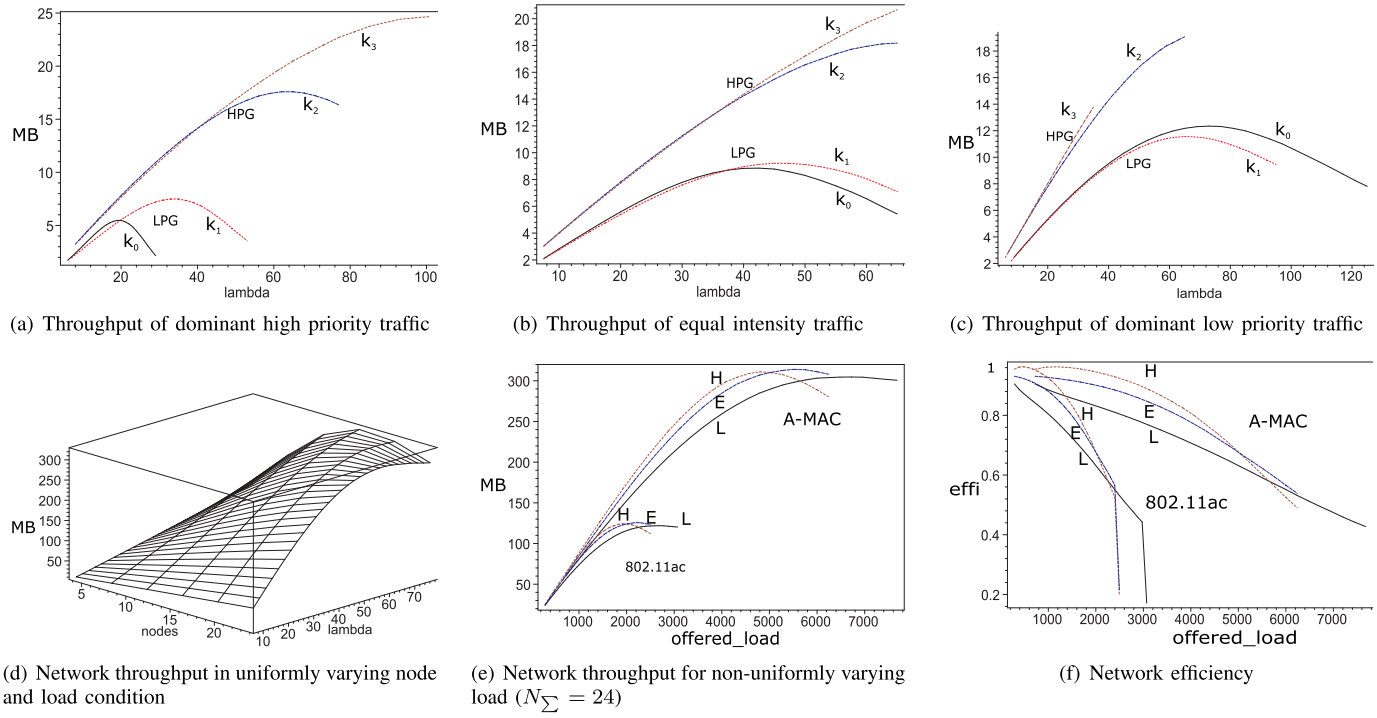

(a) Throughput of dominant high priority traffic

(b) Throughput of equal intensity traffic

(c) Throughput of dominant low priority traffic

(d) Network throughput in uniformly varying node and load condition

(e) Network throughput for non-uniformly varying load ($N_{\sum} = 24$)

(f) Network efficiency

Fig. 11. Network throughput and efficiency of A-MAC protocol.

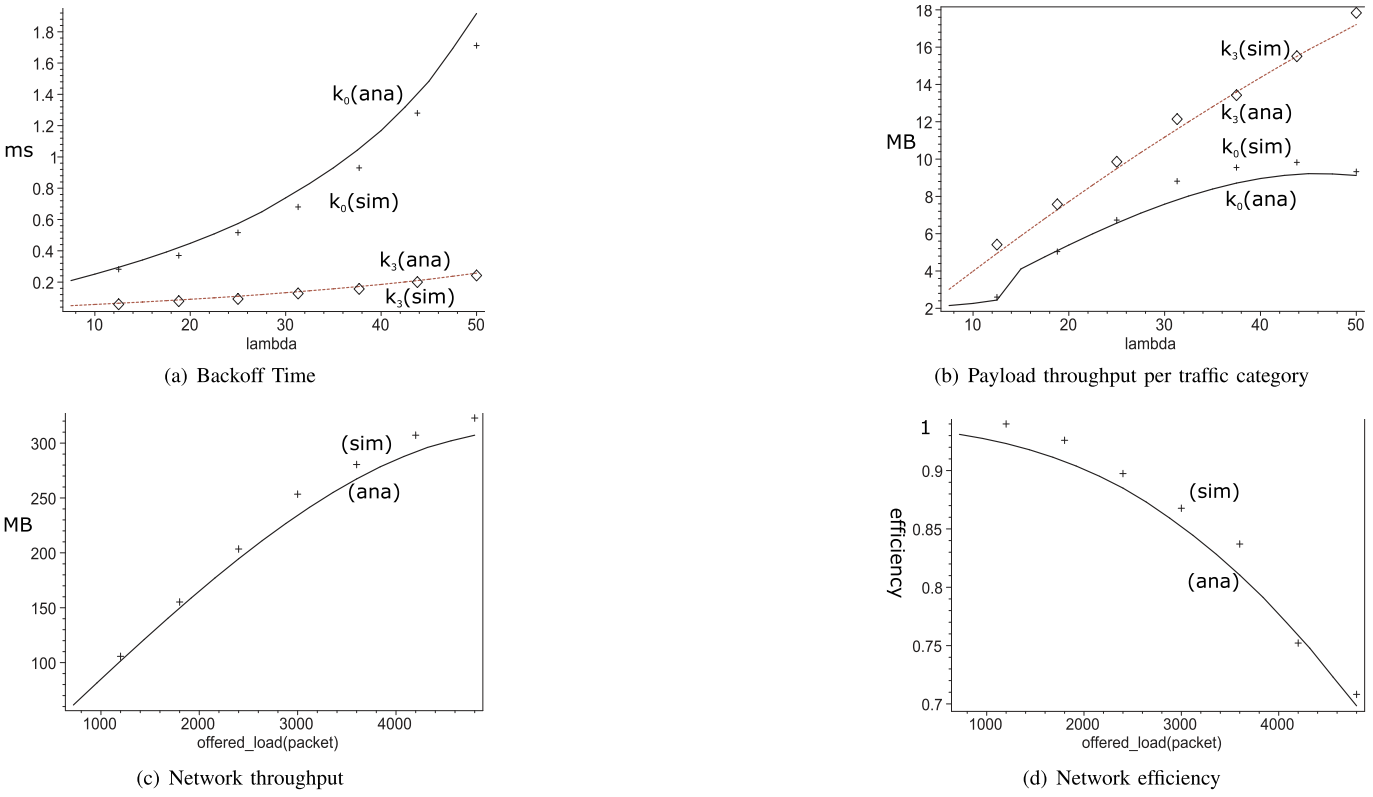

(a) Backoff Time

(b) Payload throughput per traffic category

(c) Network throughput

(d) Network efficiency

Fig. 12. Comparison of analytical model with simulation results for A-MAC.

labeled as (ana) and shown with lines, and simulation results labeled as (sim) and shown with symbols. Fig. 12(a) shows the backoff time for equal traffic intensity for all priority categories. As can be seen, the match between analytical and simulation results is quite good, with slight differences due to truncation of polynomials in the analytical model, namely in equations (19), (20) and (22), which was done to conserve memory space and prevent the Maple solver from

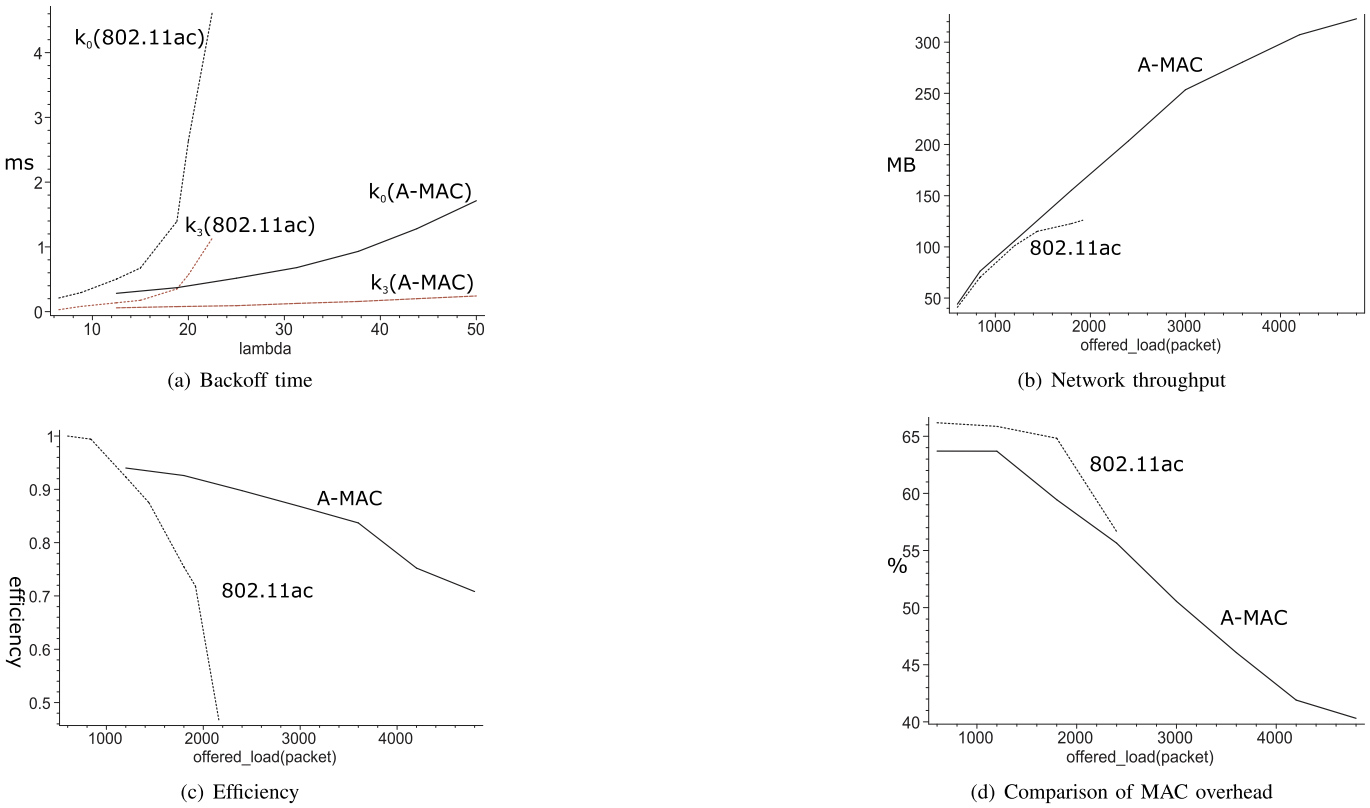

(a) Backoff time

(b) Network throughput

(c) Efficiency

(d) Comparison of MAC overhead

Fig. 13. Comparison of simulation results of A-MAC with 802.11ac protocol.

crashing due to heavy computational load. For example, at an offered load of 4200 packets/sec, the analytical model yields a network throughput of 290MB at an efficiency of 73% while the throughput obtained by simulation is about 7% higher at 310MB, with the corresponding efficiency of 75%, as shown in Fig. 12(c) and Fig. 12(d).

Performance comparison between A-MAC and 802.11ac is shown in Fig. 13, with A-MAC clearly outperforming 802.11ac in all cases. The analytical model of SU backoff time shown in Fig. 8 matches closely the SU simulation backoff time shown in Fig. 13(a). In both cases we see that at an arrival rate of 25 packets/category/node, the SU transmission reaches saturation condition and the backoff time for lower priority traffic reaches about 8ms. The backoff time for A-MAC remains within few milliseconds even at a higher packet arrival rate. Network throughput and efficiency of SU analytical model, shown in Figs. 11(e) and Fig. 11(f) respectively, are in complete agreement with the simulation results shown in Fig. 13(b) and Fig. 13(c) respectively. Fig. 13(d) shows the MAC overhead as the ratio of the amount of control message against the amount of data. At lower traffic intensity, overhead is high for both 802.11ac and A-MAC transmission. For SU transmission, more packets are transmitted during TXOP period of SU as the offered load increases which reduces MAC overhead; the lowest MAC overhead achieved in the network is 51%. For MU transmission, more packets are transmitted as secondary packets as the offered load increases; furthermore, multiple packets are transmitted during a TXOP period which further reduces MAC overhead to 38%.

802.11ac protocol allows only SU uplink transmission whereas A-MAC supports MU transmission in uplink direction. As packet arrival rate increases, more packets are queued for SU transmission and makes network unstable. However, for A-MAC protocol queue build-up takes place at much higher packet arrival rate. In this paper, we have considered only stable operating region up to onset of saturation. Onset of saturation is defined as a point where the idle probability of a STA is zero. In Figs. 11(e) and 13(b) we observe that 802.11ac network goes to saturation at an arrival rate of around 2000 packets/sec. If we further increase packet arrival rate, network becomes unstable and analytical model does not render real solution. This saturation point is also verified by simulation as shown in Fig. 13(b) where the simulator can handle around 2000 packets/sec for 802.11ac protocol at onset of saturation.

Collision probability due to hidden node is shown in Fig.14(b). At low packet arrival rate the collision probability is very low because of longer packet interarrival time and single packet transmission. The vulnerable time for collision probability due to hidden node is shorter for SU transmission and packet interarrival time is long enough to complete the transmission of RTS/CTS signaling. As the packet arrival rate increases, the packet interarrival time decreases and more MU transmissions are initiated. If a MU RTS/CTS collides with a transmission from a hidden node, multiple packets are affected and retransmission of all the affected packets are initiated which generates further collisions. Even at higher packet arrival rate, the hidden nodes form separate MU transmission

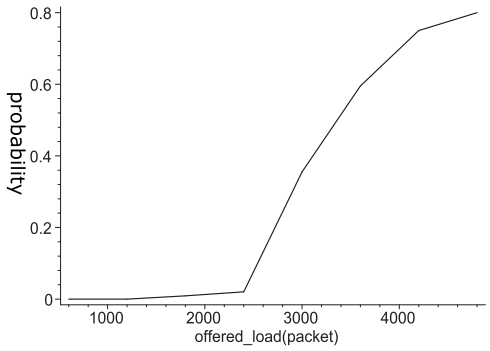

(a) Collision probability due to hidden node

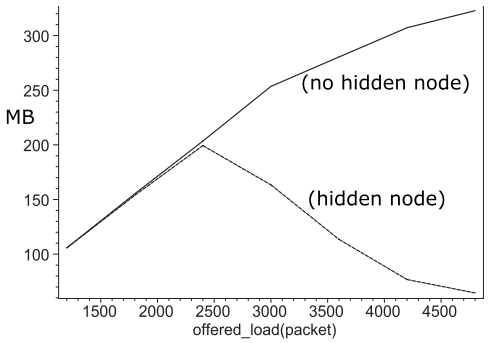

(b) Impact of hidden node on network throughput

Fig. 14. Collision probability and network throughput in presence of hidden node.

group that generates collision with another MU transmission and, consequently, the collision probability becomes very high. Fig. 14(b) shows the impact of hidden nodes on network throughput, obtained through simulation; as can be seen, hidden nodes affect the network throughput rather severely at very high packet arrival rate.

VI. Conclusion

In this paper we proposed A-MAC protocol that allowed multi-user communication in UL and we developed a detail analytical model of the proposed A-MAC protocol using M/G/1 queuing model and Markov chain model. The protocol achieved a network throughput which is 150% higher than the throughput of 802.11ac transmission for the same PHY layer capabilities. Although we achieved enhanced network throughput by increasing the intensity of higher priority traffic, we observed that network became unstable very quickly as the low priority traffic gets less opportunity to transmit. The proper selection of contention window and AIFS number (AIFSN) can ensure better network stability and fairness among all traffic categories. The proposed concurrent RTS transmission and channel sounding technique using dedicated OFDM subcarrier blocks and multiple UL transmission using MU-MIMO technique can be an important contribution for future amendment of IEEE 802.11 protocol towards 5G. Our results also showed that the network metrics for all four traffic categories could effectively be represented by two distinct priority groups which advocates in favor of the prioritization of network traffic in only two categories in the future amendment.

References

[1] Y. J. Zhang, P. X. Zheng, and S. C. Liew, "How does multiple-packet reception capability scale the performance of wireless local area networks?" *IEEE Trans. Mobile Comput.*, vol. 8, no. 7, pp. 923–935, Jul. 2009.

[2] O. Bejarano, S. Quadri, O. Gurewitz, and E. W. Knightly, "Scaling multi-user MIMO WLANs: The case for concurrent uplink control messages," in *Proc. 12th Annu. IEEE Int. Conf. Sens., Commun., Netw. (SECON)*, Jun. 2015, pp. 238–246.

[3] A. Sibille, C. Oestges, and A. Zanella, *MIMO: From Theory to Implementation*. New York, NY, USA: Elsevier, 2010.

[4] T. Brown, P. Kyritsi, and E. De Carvalho, *Practical Guide to MIMO Radio Channel*. Hoboken, NJ, USA: Wiley, 2012.

[5] C. B. Papadias and A. J. Paulraj, "A constant modulus algorithm for multiuser signal separation in presence of delay spread using antenna arrays," *IEEE Signal Process. Lett.*, vol. 4, no. 6, pp. 178–181, Jun. 1997.

[6] S. Talwar, M. Viberg, and A. Paulraj, "Blind separation of synchronous co-channel digital signals using an antenna array. I. Algorithms," *IEEE Trans. Signal Process.*, vol. 44, no. 5, pp. 1184–1197, May 1996.

[7] J. Qiu *et al.*, "Hierarchical resource allocation framework for hyper-dense small cell networks," *IEEE Access*, vol. 4, pp. 8657–8669, 2016.

[8] J. Qiu, Q. Wu, Y. Xu, Y. Sun, and D. Wu, "Demand-aware resource allocation for ultra-dense small cell networks: An interference-separation clustering-based solution," *Trans. Emerg. Telecommun. Technol.*, vol. 27, no. 8, pp. 1071–1086, 2016.

[9] S. Ghez, S. Verdú, and S. C. Schwartz, "Stability properties of slotted aloha with multipacket reception capability," *IEEE Trans. Autom. Control*, vol. AC-33, no. 7, pp. 640–649, Jul. 1988.

[10] L. Tong, Q. Zhao, and G. Mergen, "Multipacket reception in random access wireless networks: From signal processing to optimal medium access control," *IEEE Commun. Mag.*, vol. 39, no. 11, pp. 108–112, Nov. 2001.

[11] Q. Zhao and L. Tong, "A dynamic queue protocol for multiaccess wireless networks with multipacket reception," *IEEE Trans. Wireless Commun.*, vol. 3, no. 6, pp. 2221–2231, Nov. 2004.

[12] P. X. Zheng, Y. J. Zhang, and S. C. Liew, "Multipacket reception in wireless local area networks," in *Proc. IEEE Int. Conf. Commun.*, vol. 8, Jun. 2006, pp. 3670–3675.

[13] S. Zhou and Z. Niu, "An uplink medium access protocol with SDMA support for multiple-antenna WLANs," in *Proc. IEEE Wireless Commun. Netw. Conf.*, Mar./Apr. 2008, pp. 1809–1814.

[14] K. Tan *et al.*, "SAM: Enabling practical spatial multiple access in wireless LAN," in *Proc. 15th Annu. Int. Conf. Mobile Comput. Netw. (MobiCom)*, New York, NY, USA, 2009, pp. 49–60.

[15] T. Tandai, H. Mori, K. Toshimitsu, and T. Kobayashi, "An efficient uplink multiuser MIMO protocol in IEEE 802.11 WLANs," in *Proc. IEEE 20th Int. Symp. Pers., Indoor Mobile Radio Commun.*, Sep. 2009, pp. 1153–1157.

[16] F. Babich and M. Comisso, "Theoretical analysis of asynchronous multi-packet reception in 802.11 networks," *IEEE Trans. Commun.*, vol. 58, no. 6, pp. 1782–1794, Jun. 2010.

[17] D. Jung, R. Kim, and H. Lim, "Asynchronous medium access protocol for multi-user MIMO based uplink WLANs," *IEEE Trans. Commun.*, vol. 60, no. 12, pp. 3745–3754, Dec. 2012.

[18] C. Chen, S. Hou, and S. Wu, "A novel analytical model for asynchronous multi-packet reception MAC protocol," *IEEE Commun. Lett.*, vol. 21, no. 6, pp. 1289–1292, Jun. 2017.

[19] H. Li, A. Attar, and V. C. M. Leung, "Multi-user medium access control in wireless local area network," in *Proc. IEEE Wireless Commun. Netw. Conf.*, Apr. 2010, pp. 1–6.

[20] Y. J. Zhang, "Multi-round contention in wireless LANs with multipacket reception," *IEEE Trans. Wireless Commun.*, vol. 9, no. 4, pp. 1503–1513, Apr. 2010.

[21] R. Lio, B. Bellalta, T. M. Cao, J. Barcelo, and M. Oliver, "Uni-MUMAC: A unified down/up-link MU-MIMO MAC protocol for IEEE 802.11ac WLANs," *Wireless Netw.*, vol. 21, no. 5, pp. 1457–1472, 2014.

[22] M. Z. Ali, J. Mišić, and V. B. Mišić, "Performance analysis of downlink MU-TXOP sharing in IEEE 802.11ac," *IEEE Trans. Veh. Technol.*, vol. 66, no. 10, pp. 9365–9380, Oct. 2017.

[23] J. Mišić, S. Rashwand, and V. B. Mišić, "Analysis of impact of TXOP allocation on IEEE 802.11e EDCA under variable network load," *IEEE Trans. Parallel Distrib. Syst.*, vol. 23, no. 5, pp. 785–799, May 2012.

[24] H. Takagi, *Queueing Analysis: Discrete-Time Systems v.3: A Foundation of Performance Evaluation: 003*. Amsterdam, The Netherlands: North Holland, 1993.

M. Zulfiker Ali (S'17) received the B.A.Sc. degree in electrical and electronic engineering from the Bangladesh University of Engineering and Technology, Dhaka, Bangladesh, in 1995, and the M.A.Sc. degree in electrical and computer engineering from Ryerson University, Toronto, ON, Canada, in 2013, where he is currently pursuing the Ph.D. degree. His research interests include wireless communications and its applications, Internet of Things, and VANETs.

Jelena Mišić (M'91–SM'08–F'18) is currently a Professor of computer science with Ryerson University, Toronto, ON, Canada. She has published over 120 papers in archival journals and nearly 200 papers at international conferences in the areas of wireless networks, particular wireless personal area network and wireless sensor network protocols, performance evaluation, and security. She is a member of ACM. She serves on the Editorial Boards of the IEEE TRANSACTIONS ON VEHICULAR TECHNOLOGY, *Computer Networks*, *Ad hoc Networks*, *Security and Communication Networks*, *Ad Hoc & Sensor Wireless Networks*, the *International Journal of Sensor Networks*, and the *International Journal of Telemedicine and Applications*.

Vojislav B. Mišić (M'92–SM'08) received the Ph.D. degree in computer science from the University of Belgrade, Serbia, in 1993. He is currently a Professor of computer science with Ryerson University, Toronto, ON, Canada. His research interests include performance evaluation of wireless networks and systems and software engineering. He has authored or co-authored six books, 20 book chapters, and over 280 papers in archival journals and at prestigious international conferences. He is a member of ACM. He serves on the Editorial Boards of the IEEE TRANSACTIONS ON CLOUD COMPUTING, *Ad hoc Networks*, *Peer-to-Peer Networking and Applications*, and the *International Journal of Parallel, Emergent and Distributed Systems*.